Review and data evaluation for high-temperature reduction of iron oxide particles in suspension

Zhiyuan Chen , Christiaan Zeilstra , Jan van der Stel , Jilt Sietsma & Yongxiang Yang

The Institute of Materials,
Minerals and Mining

Taylor & Francis
Taylor & Francis Group

REVIEW

Review and data evaluation for high-temperature reduction of iron oxide particles in suspension

Zhiyuan Chen [a], Christiaan Zeilstra[b], Jan van der Stel[b], Jilt Sietsma[a] and Yongxiang Yang [a]

[a]Department of Materials Science and Engineering, Delft University of Technology, Delft, Netherlands; [b]R&D Ironmaking, Tata Steel, IJmuiden, Netherlands

ABSTRACT

High-temperature reduction processes of iron oxide particles suspension are promising in carbon emission abatement. Recently, researchers have contributed abundant knowledge of the reaction mechanism and kinetics of iron oxide particles above 1473 K, while there was very limited information 10 years ago. Although the understanding of the high-temperature reduction of iron oxide particles is still not comprehensive, a brief review of the academic reports is helpful for the future work on this topic. The high-temperature reduction of iron oxide suspension is characterized by having: rapid reaction, obvious thermal decomposition and melting process. Evaluation of the kinetic data shows that the reduction process of single particles is not rate-determined by the diffusion process at the studied temperatures. The reaction rate constant is within 10^{-2}–10 s^{-1} in these studies. Furthermore, comparing previous studies in iron oxide reduction field, the phase transformation and effect of gangue minerals to the reduction of iron oxide particles above 1473 K requires more input and research.

Introduction

Nowadays, reducing CO_2 emission is one of the most important tasks of the ironmaking industry. To cut down CO_2 emission, technological innovation of the production process is critical for the industry. The European Union supports the development of HIsarna as an emerging alternative ironmaking process. As a part of ULCOS (Ultra-Low CO_2 Steelmaking) programme [1], a reduction up to 80% CO_2 by HIsarna is investigated by Tata Steel, IJmuiden. HIsarna uses a smelt cyclone for iron ore pre-reduction and a smelting reduction vessel for final reduction. Fine iron oxide particles are injected into the smelt cyclone, pre-reduced and molten in suspension. After hitting the wall of the reactor, the melt falls into the smelting reduction vessel underneath. The temperature of the reacting gas in the cyclone can be up to about 1673–2273 K. Recently, in the USA, an alternative suspension reduction process of magnetite ore particles has been proposed by Sohn [2] with the support of AISI steel industry participants and US Department of Energy. In that reactor, iron oxide concentrates were directly reduced by gaseous reducing agents. The reaction temperature reached 1673 K [3] and even higher. A considerable CO_2 emission reduction and energy saving are expected for this process [4]. Both processes are based on the (partial) reduction in suspension of fine iron oxides at high temperature. The suspension reduction is defined as 'the direct gaseous reduction of fine ore concentrates which are transported by gases', which is modified from the definition by Park and Jung [5]. Moreover, researchers are developing other sustainable metallurgical processes based on high-temperature suspension reduction technologies as well. Xu et al. [6,7] studied the reduction behaviour of blast furnace dust during the suspension

reduction process to explore the possibility of this technology in treating solid wastes.

To optimize all of these high-temperature processes, fundamental data of reduction kinetics, as critical information, is essential and necessary. Phase transformation processes and the effect of other minerals to the reduction are also important. However, the reduction of iron oxide particles at such high temperature is rarely discussed and summarized in the previous reports. The purpose of this paper is to provide a brief review and overall evaluation of recent works on the reduction in suspension of iron oxides, with the comparison of previous studies at lower temperatures.

Phase transformation

It is well known that the reduction of pure haematite follows three steps: $Fe_2O_3 \rightarrow Fe_3O_4 \rightarrow FeO \rightarrow Fe$. The corresponding reduction degrees are $0\% \rightarrow 11\% \rightarrow 33\% \rightarrow 100\%$, respectively. Here, the reduction degree is defined as the ratio of the loss of oxygen in the reduction to the total content of oxygen in haematite. At a specified temperature, the termination of the reaction is expected to be the equilibrium state to achieve the highest utilization of reducing gas. Therefore, reduction analysis is always based on the equilibrium diagram of the Fe–O system [8,9]. Temperature and gas composition are the two important factors to the equilibrium state of iron oxides. For complex gas mixtures, PCR (post combustion ratio, which is defined as $(CO_2\% + H_2O\%)/(CO\% + H_2\% + CO_2\% + H_2O\%)$ in volume) is particularly used to characterize gas composition in industry. The equilibrium reduction degree of iron oxides is inversely proportional to the PCR value. A decrease of PCR value from 85% to 36% could promote the reduction degree of iron oxides from 23.3% to

CONTACT Zhiyuan Chen ✉ aha_c@126.com 🖂 Department of Materials Science and Engineering, Delft University of Technology, Mekelweg 2, 2628 CD Delft, Netherlands

29.7% at 1650 K [10]. The reduction from haematite to magnetite only needs a very low concentration of reducing gas according to the equilibrium diagram of Fe–O system. Especially, haematite thermally decomposes to magnetite in an inert gas or even in an oxidizing gas at high temperature. The decomposition becomes obvious from around 1500 K [11]. Therefore, it comes to the first characteristic of the reduction of haematite particles at high temperature, which contains two parts: thermal decomposition and chemical reduction above 1500 K.

Thermal decomposition is the principal reaction at the initial 202 ms, during which time the reduction degree reaches about 3–11% in a high-temperature drop-tube furnace from 1650 to 1800 K under inert gas condition [11]. This result indicates that the reaction during thermal decomposition of haematite is principally the reduction from haematite to magnetite. Accordingly, the chemical reduction is mainly the reduction from magnetite to wüstite. According to the result, one could know the second characteristic of the reduction of haematite particles at high temperature that the reaction can be fast enough to reach the reaction end point within seconds around 1750 K [12].

Since the melting point of wüstite is 1650 K, which is much lower than haematite and magnetite, the particles start melting when wüstite forms in the reaction. With other minerals inside the ore, the liquidus temperature of the ore could be even lower. The research from Qu et al. [10] uncovered the melting behaviour of the reduced iron oxides in the experiments. A complete melting down of all particles was observed at 1700 K when the particle residence time was above 970 ms. It comes to the third characteristic that reduction of iron oxides accompanies melting above 1650 K.

Among the above three characteristics, the first and the third one can be predicted from the thermodynamic diagram of Fe–O system (Figure 1). Besides, it is noted that in this thermodynamic diagram there are three predominant areas for lath magnetite [13–15], and dense and fibrous metallic iron [16]. The three products mentioned above have not been taken into consideration at high temperatures (>1500 K) for the reason that, experimentally, the lath magnetite was observed below 1473 K with low reducing potential [13,17], layered-dense iron between 873 and 1023 K, and fibrous iron between 973 and 1273 K [16,18]. Hereby, it is expected that only porous magnetite and porous iron would form in
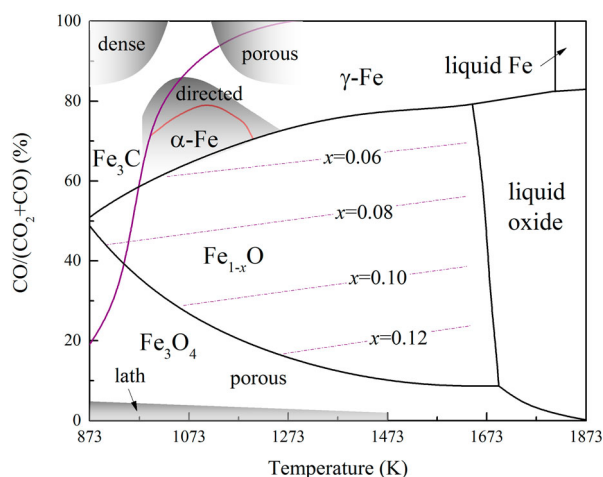
the reduction at a high temperature above 1273 K. By the way, fibrous iron is well known for causing swelling of iron ore pellets [19] and sticking of particles [20]. The possibility of agglomeration of iron oxide particles by the hookup of fibrous iron in high-temperature drop-tube furnace or smelting cyclone reactor is expected to be unlikely according to the above analysis. In a special case, Seaton et al. [21] claimed that 'dendritic like' iron filamentary was found at a temperature higher than 1273 K, which requires further verification.

At high temperature, besides solid phase transformation, melting produces a matte surface of the particles with the molten products as mentioned before. External mass transfer controls the overall rate of the reaction when the particle temperature is above the melting point, while it is controlled by the intrinsic kinetics below the melting point [23]. The liquid slag could block pores and then decrease the reduction process. Nakamoto et al. [24] found that during the reduction of FeO, compact, smaller pores were blocked first thereby slightly decreasing the reducibility. However, the reducibility got much worse when the larger pores were filled with liquid slag.

Different from the pure haematite, minor contents of gangue minerals are present in commercial ore particles. It could result in different phase transformation mechanisms during the reduction process, which further affects the melting behaviour and reduction kinetics. The phase transformation mechanism contains two aspects, the reduction sequence and the characteristics of the topochemical reduction interface. Maeda and Ono [25] studied the reduction sequence and reduction equilibrium of $CaO–Fe_2O_3–Al_2O_3$ ternary calcium ferrite with $CO–CO_2$ mixture. It was found that a higher equilibrium CO content is needed to reduce the 2 mass% Al_2O_3 containing calcium ferrite than the $CaO–Fe_2O_3$ binary to reach the same reduction degree, but no obvious difference between their crystal structures was found. For the $CaO–Fe_2O_3$ binary, many intermediate products, such as $CaO·FeO·Fe_2O_3$, $CaO·3FeO·Fe_2O_3$, FeO and $2CaO·Fe_2O_3$, were formed in the reduction process. However, in the quaternary calcium ferrite, $CaO–Fe_2O_3–SiO_2–Al_2O_3$, it forms an iron oxide phase based solid solution rather than intermediate complex oxides [26]. It could be due to the complex interaction of different phases present in the ore.

Usually, the topochemical reaction in the form of the reduced shell covering on the un-reacted core is one of the most frequently observed phenomena in studies, regardless of the reaction temperature [12,27]. Shrinkage of the un-reacted core is accompanied by increasing reduction degree in this process. A kinetic model can be established based on the inward moving of the chemical reaction interface in the particle. In contrast, if the reduced phase is dispersed throughout the particle, the kinetic model should be different [28–30]. At last, the melting process also will lead to a series of issues to be studied. The SEM photos of reduced molten wüstite in CO gas showed that metallic iron parts are dispersed in the unreduced part [31–33], where the appreciable diffusion resistances of species in the molten slag phase needs to be considered in the kinetic analysis. Furthermore, the interface of the reduced core is moving outward during the reaction, which implies a different kinetic mechanism.

Figure 1. Predominant phase diagram of iron oxide in CO-CO$_2$ atmosphere [12,15,22].

Iron oxides suspension reduction kinetics

While there are many studies on the reduction from wüstite to iron [31–38] and reduction of iron oxides from 673 to 1473 K,

this work focusses on the suspension reduction process of haematite and magnetite above 1473 K for emerging alternative ironmaking processes. A reaction kinetics study is a basis for a study of the whole reaction process. For instance, a computational fluid dynamics (CFD) study is the principal method to optimize the parameters of reactor and operation process, and reduction kinetic formula and related parameters are critically needed for successful CFD studies [39–42].

Usually, the kinetic model of reactions would change with increasing temperature. At low temperature, e.g. the study of Gao et al. [43] on the reduction of haematite in H_2 and CO (temperature range was from 873 to 1373 K) indicates that the internal mass transfer is the reaction rate determining step. However, it is rare to be proposed as the rate-determining step above 1473 K.

As mentioned in the previous section, the reduction of haematite above 1650 K contains thermal decomposition and chemical reduction. A kinetic study of Salmani et al. [44] on thermal decomposition of haematite particles indicated that haematite could be thermally decomposed to magnetite in either inert gas and air atmosphere. They suggested the apparent activation energy of the reaction to be 324 and 382 kJ/mol in inert gas and air atmosphere based on the thermogravimetric results, respectively. The experimental results of differential scanning calorimetry indicated a higher value for the reaction process: 424 and 594 kJ/mol in inert gas and air atmosphere, respectively. The chemical reaction was proposed to be the reaction rate-determining step in his work. Unfortunately, to the knowledge of the authors, there is no more experimental study on kinetic analysis of thermal decomposition.

Qu et al. [12,45] studied the chemical reduction rate of haematite from 1550 to 1750 K. The reaction rate determining step of both solid–gas reaction below 1650 K and liquid–gas reaction above 1650 K is the interfacial chemical reaction. Their study also indicated a linear relationship of the rate constant of solid–gas reaction to the partial pressures of CO and H_2. Moreover, the relationship of reaction rate constant of solid–gas reaction with temperature is as follows:

$$k = 9.36 \times 10^6 \exp\left(\frac{-2.70 \times 10^5}{RT}\right), \tag{1}$$

where the k is the rate constant, R is the gas constant (8.314 J/mol/K), and T is the temperature in K. It shows that

the reaction activation energy is 270 kJ/mol. Based on this value, they suggested that the rate determining step in the view of micro-kinetics should be the mass transport of cations and electrons along the reaction interfaces. The activation energy of liquid–gas reaction has not been reported in their publication, but the rate of it has been proposed to be of the order of 10^{-2} s^{-1} [12,45].

Choi [3,46] studied the hydrogen reduction of magnetite concentrate in suspension (25–32 μm) at different temperatures. According to his prediction, the complete reduction time of a magnetite particle with $\Phi = 15$ μm would be around 10^{-3} s at 1473 K if the reaction rate determining step is external or internal mass transfer. Based on the calculation result, he suggested that the reduction rate of iron ore concentrate from 1473 to 1673 K was controlled by a chemical reaction. He found a curious phenomenon that the dependence of reduction rate on temperature between 1673 and 1773 K was weaker than that in the lower temperature range. He implied this to be the effect of particle morphology variation. It is compatible with the analysis of Nakamoto et al. [24]. Moreover, it was expected that higher temperature would heavily elevate the reaction rate due to the full melting of particles [3,46].

Unfortunately, he did not report the reaction rate constant. Therefore, the data of the reduction degree in his thesis was reanalyzed in this review to figure out the kinetic parameters. WebPlotDigitizer 3.10 developed by A. Rohatgi was employed to extract data from the published figures. The un-reacted core shrinking model (UCSM) [29,47] was used for the kinetic analysis in order to keep consistent with Qu's analysis result [12,45]:

$$1 - (1 - x)^{1/3} = kt, \tag{2}$$

where x is the reduction degree and t is time in s. The result (see Figure 2) shows that the model fits the experimental data very well. '% excess H_2' in the figure means the amount of hydrogen fed into the reactor other than the minimum amount of hydrogen for complete reduction of magnetite to metallic iron. One could notice that some series of data contains only two points (exclude the origin), which may result in larger calculation error for the reaction rate constants. Owing to a lack of data at 1773 K, the corresponding reaction rate constant could only be estimated to be lower than 0.765 s^{-1}. The Arrhenius formula is employed to calculate
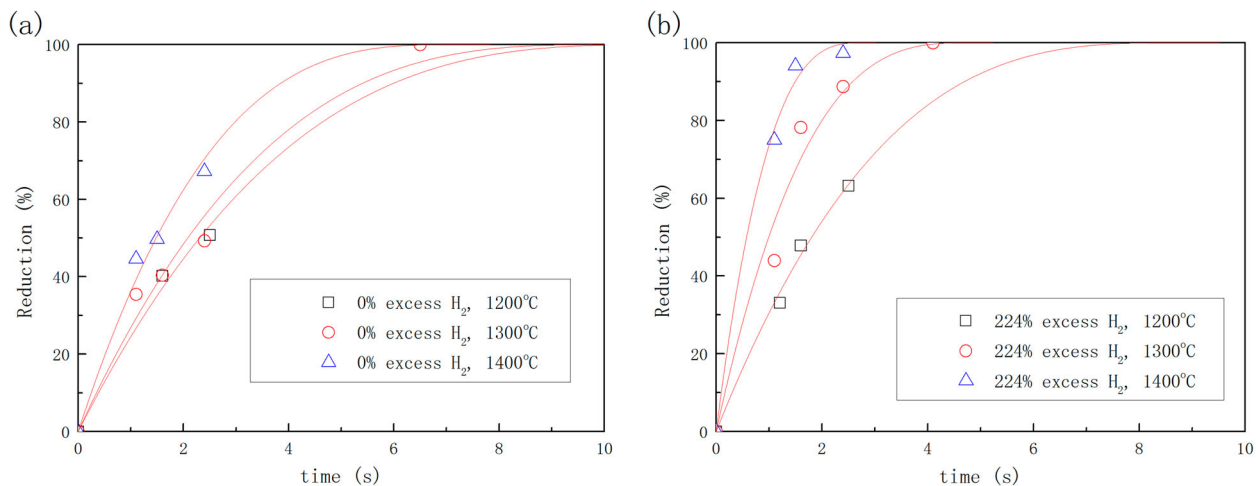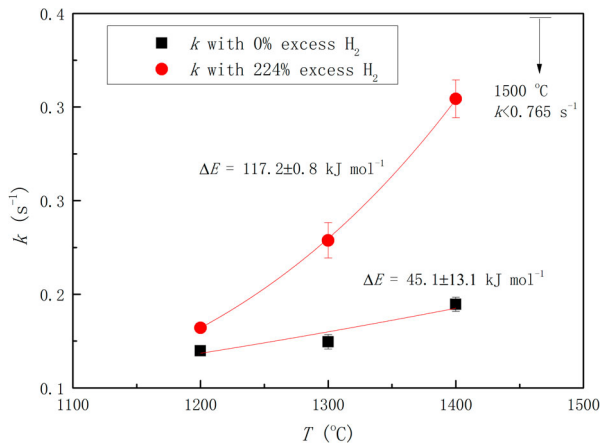
Figure 2. Hydrogen reduction rate of magnetite concentrate in high-temperature drop-tube reactor system (0.85 atm).

Figure 3. Reaction rate constants of magnetite concentrate in high-temperature drop-tube reactor system (0.85 atm).

the apparent activation energy of the reduction. As shown in Figure 3, it indicates that the value of apparent activation energy varies with different % excess hydrogen. The reason could be that relatively high content of water vapour in 0% excess hydrogen depressed the reducing potential in the surrounding atmosphere of the ore significantly. Moreover, the reducing potential kept decreasing along with the reduction process. This decreasing rate was higher when the reaction rate was faster at a higher temperature, working as negative feedback to the reaction rate. As a result, the apparent activation energy, which is the effect of temperature on the reaction rate, has been reduced to be 45.1 ± 13.1 kJ mol^{-1}. Therefore, we recommend the data with 224% excess hydrogen as the apparent activation energy of magnetite in pure hydrogen, which is 117.2 ± 0.8 kJ mol^{-1}.

Wang [48,49] continued Choi's work on the study of magnetite concentrate. A detailed kinetic analysis was carried out in his thesis. He suggested the reduction kinetics of ore in suspension above 1423 K should be:

$$[-\ln(1-x)]^{1/2} = 9.9 \times 10^{14} \exp(4.63 \times 10^5/RT)[p_{H_2}^{1/2}$$
$$- (p_{H_2O}/K)^{1/2}]d^s t, \qquad (3)$$

where,

$$s = \frac{2.73 \times 10^8}{T^2} - \frac{345930}{T} + 109.5 \quad T = 1423 \sim 1573K,$$
$$s = 0 \quad T \geq 1573K, \qquad (4)$$

where p is pressure in reactor atmosphere in atm, d is mean size of particles in μm, T is in K, t is in s, and K is the equilibrium constant for hydrogen reduction of FeO under the assumption that the reduction from FeO to Fe is equilibrium-limited.

This equation is a nucleation and growth model with Avrami parameter of $n = 2$. According to Equation (3), the activation energy of the overall reaction was determined to be 463 kJ mol^{-1}. This value is much higher than the one calculated on basis of the data of Choi (being 117.2 kJ mol^{-1}) because different models were employed in the calculation. The effects of particle size, hydrogen partial pressure, equilibrium constant and temperature are included in this equation. For high % excess hydrogen ambience, the influence of equilibrium constant could be ignored. It should be noticed that the content of gangue varied with the change of particle size in the experiment, which could

be one of the principal reasons of the increase of reaction rate with the particle size at low temperatures as Equation (4) shows [48,49].

The reduction kinetics of magnetite concentrate particles in hydrogen was suggested to be similar to the mechanism in the work of Fan et al. [39]. The suspension reaction temperature was from 1423 to 1623 K. The model was proposed to be nucleation equation with Avrami parameter of $n = 1$ and activation energy of 196 kJ mol^{-1}. The partial pressure of hydrogen and water vapour to the apparent reaction rate constant was suggested to be with a linear relationship. Elzohiery et al. [50] reported the same kinetic equation with an activation energy of 193 kJ mol^{-1}. In another study of Fan et al. [40], the same kinetic mechanism was recommended for both H$_2$ and CO gases, with reported activation energy from Chen et al. [51–53] of 214 and 231 kJ mol^{-1} from 1473 to 1623 K for H$_2$ and CO, respectively.

Abolpour et al. [54] reported the reduction kinetics of magnetite ore concentrate in a crucible at the temperature from 973 to 1173 K as follows:

$$[-\ln(1-x)]^{1/1.078} = 3.27 \times 10^{-3}d_p^{-1.871}C_{CO}^{2.738} \exp$$
$$(-2.438 \times 10^5/RT)t, \qquad (5)$$

where d_p is the diameter of the particle in μm, C_{CO} is the concentration of CO in atm. This equation is similar to the Avrami form, with 'Avrami' parameter of 1.078. Accordingly, the activation energy was 243.8 kJ mol^{-1}.

In the following experimental study of Abolpour et al. [41] of suspension reduction of magnetite concentrate by a CO and Ar mixture, the kinetic model was also suggested to obey a similar equation of $[-\ln(1-x)]^{1/n}$ with $n = 0.56$. The activation energy was proposed to be 219.6 kJ mol^{-1} for the reaction.

Wang and Sohn [48,55] also studied the suspension reduction of magnetite concentrate with 32–38 μm in CO containing atmosphere under 0.85 atm. Only the experimental data with 800% excess H$_2$ was collected from their work for analysis in that the effect of water vapour could be neglected. Both the un-reacted core shrinking model (chemical reaction controlled) and the Avrami equation ($n = 2$) were employed for analysis. As shown in Figure 4, however, both models are not satisfying. All reaction rate constants were listed in Table 1. The unsatisfying results could be the influence of heat transfer and fluid flow in the reactor. Therefore, CFD studies of suspension reduction [39–42] were reported in recent years.

Park and Jung [5] investigated the suspension reduction behaviour of Chinese Benxi magnetite ore particles at high temperatures. The reaction kinetics were described by an un-reacted shrinking core model. The activation energy of magnetite reduction was recommended to be 76.9 kJ mol^{-1} in 20 vol.-% H$_2$ within 1423 and 1573 K based on the assumption that the reaction is controlled by chemical reaction. The experimental result showed that the reduction rate of magnetite ore in H$_2$ was higher than that in CO, both of which were lower than in CH$_4$. CH$_4$ is supposed to not only provide carbon as reducing agent but also provide H$_2$ (here we suppose that H(ad) can react with iron in the oxidation state directly) by cracking in the reduction. Since the reduction of magnetite to wüstite was much faster than wüstite to metallic iron, they assumed the overall reaction rate is determined by the chemical reaction from wüstite to iron. For this reason, they
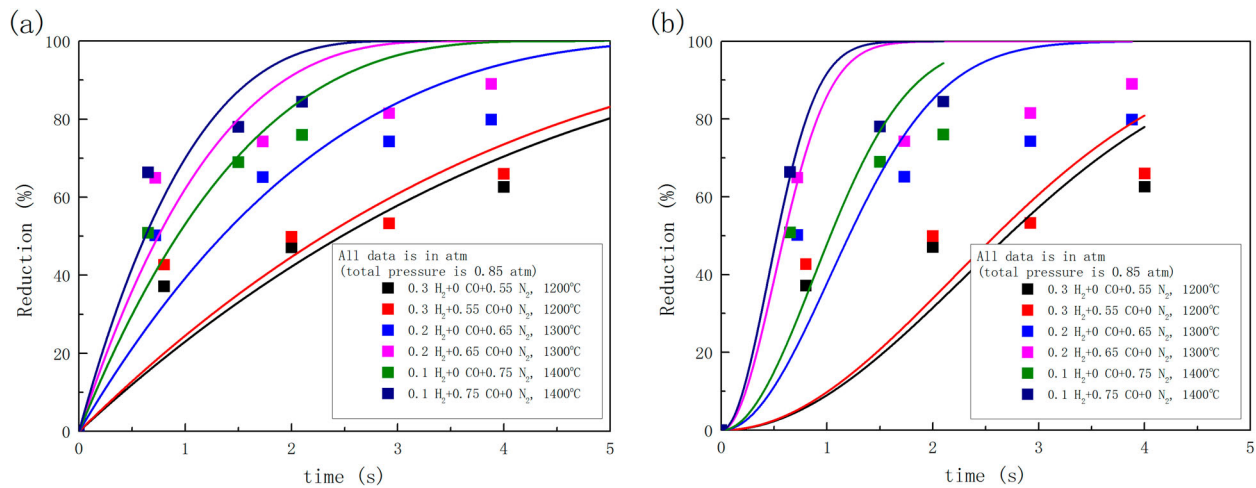
Figure 4. Reduction kinetics of magnetite concentrate particles with prediction of (a) un-reacted core shrinking model (chemical reaction controlled) and (b) Avrami equation ($n = 2$).

Table 1. Reaction rate constant used for prediction in Figure 4.

Temp.(°C)	1473		1573		1673	
H_2:CO:N_2	0.3:0:0.55	0.3:0.55:0	0.2:0:0.65	0.2:0.65:0	0.1:0:0.75	0.1:0.75:0
UCSM (s^{-1})	0.0835 ± 0.0121	0.0895 ± 0.0154	0.153 ± 0.029	0.277 ± 0.072	0.223 ± 0.031	0.331 ± 0.071
Avrami ($n = 2$) (s^{-1})	0.308 ± 0.053	0.322 ± 0.062	0.690 ± 0.188	1.40 ± 0.32	0.808 ± 0.182	1.58 ± 0.33

were inclined to compare his results with reported data on wüstite reduction. According to this assumption, the reduction kinetics from magnetite to wüstite is hard to observe in pure reducing gas atmosphere, but only in a gas mixture with lower reducing potential that can control the final product to be wüstite. It could also be noted that a comprehensive experimental analysis of the reduction step from magnetite to wüstite needs further experimental verification.

Xu et al. [6] applied the suspension reduction technology to recycle blast furnace dust. The XRD pattern showed that the dust mainly contained haematite, wustite, metallic iron and calcium ferrite. Their study shows that the reaction rate of gas-molten particles is determined by both the diffusion in the product layer and the interfacial chemical reaction at 1673–1723 K. It is reported that the chemical reaction constant is in the 10^{-3} m s^{-1} range, and the diffusion coefficient is in the 10^{-9} m^2 s^{-1} range.

Effect of gangue to the reduction kinetics

There are limited reports regarding the effect of gangue on the reduction kinetics of iron oxides in suspension. Therefore, solid–gas reaction below 1473 K and the slag-gas reaction at high temperature were reviewed to find the common mechanism.

The main accessory minerals in iron oxides are SiO_2, $CaMg$ $(CO_3)_2$, $CaCO_3$ and Al_2O_3. Carbon dust or fluxes could be gangue in the raw material. Nagasaka et al. [56] summarized the reaction rate of CO gas and liquid slag containing iron oxide in their work. Because the particle melts when the temperature is high enough, the reaction between slag and gas is helpful to understand the suspension reduction. The experimental data suggested that some components can decrease the iron oxide reduction rate in slag, for example, $P_2O_5 > SiO_2 > TiO_2$ with P_2O_5 having the strongest effect. On the contrary, Na_2O and CaO improve the reaction rate. Al_2O_3, MgO and MnO were reported to have no significant effect on the

reduction rate due to their limited solubility in liquid iron oxide. All these indicated that the basicity of slag is one of the important factors to the kinetics of a molten particle. Moreover, it was reported that the following equation could be used for the reduction kinetics of slag in CO gas except for P_2O_5 containing binary:

$$dx/dt = k(p_{CO} - p_{CO^2}/K)(\text{kg} - \text{oxygen/m}^2\text{s}), \quad (6)$$

$$k = k_{r,CO}(N^2_{FeO_{1.5}}/N^3_{FeO})^{1/3}, \quad (7)$$

$$k_{r,CO} = \exp(-138000/RT - 6.37)(\text{kg} \times \text{m}^{-2}\text{s} \times \text{Pa}), \quad (8)$$

where k is the apparent chemical reaction rate constant, K is the gas ratio of (p_{CO}/p_{CO_2}) in an equilibrium state. The chemical reaction rate of iron oxide containing slag in H_2 also obeys Equation (7). Like the reaction in CO, CaO improves the reduction of iron oxide in slag and SiO_2 depresses the reduction in H_2 gas. The study of Hayashi and Iguchi [33] on the suspension reduction of liquid wüstite particles also shows the same result: CaO promotes the reaction rate, SiO_2 lowers it, and Al_2O_3 has no effect on it.

EL-Geassy has done a series of works on the effect of dopants on the reduction kinetics and mechanism of iron oxide reduction as the ore in the solid state. He suggested that the increasing NiO content in oxide significantly improves the reduction rate. Total porosity increased from 6.2% to 13.4% the maximum. Here, $NiFe_2O_3$ and Ni_xFe_y were found as reactant and product, respectively. At last, the kinetic mechanism also was changed with different NiO content. These three reasons contributed to the acceleration of the reduction rate[57]. The reaction temperature was controlled within 1173–1473 K, with 1–10 mass% NiO. The effect of MgO was also studied in the range of 0.5–5.0 mass% in CO gas at the same temperature. Although the disorder in haematite lattice and the porosity increased with MgO content, the presence of MgO in haematite showed slight effects on the reduction rate below the reduction degree of 25% [58].

El-Geassy [59] found that the addition of CaO and MgO to haematite promotes the reduction rate from Fe_2O_3 to Fe_3O_4. The reaction is at 1173–1473 K, where the CaO and MgO were 1 mass%, respectively. The positive effect of MgO was suggested to be stronger than CaO. Two reasons were raised: the first is the porosity and pore size increase, second is the increasing active centres due to the intrusion of additional cations in iron oxides. The study on MnO_2 doped haematite [60] indicated that the presence of MnO_2 could promote the reduction within 1198–1373 K within 0–6 mass% MnO_2 content in CO. $MnFe_2O_4$ was detected in the raw materials, which is hardly reduced but always accompanied with large pores between grains. The destruction of $MnFe_2O_4$ within this temperature range was indicated to be the principle reason of its positive effect on swelling of compacts and then promoting the reduction rate. But such benefit is not expected above 1373 K, where the swelling is negligible. Unlike MnO_2 doped samples, EL-Geassy et al. [61] did not find new phases in 2.7–7.5 mass% SiO_2 doped haematite. Moreover, a relatively smaller swelling was detected in the presence of SiO_2. A positive effect of SiO_2 to the initial reduction rate was observed, which was the result of the original porosity of the annealed samples increased with SiO_2 content. However, the formation of hardly reducible Fe_2SiO_4 slowed down further reduction. With additional MnO_2 dopant, the formed $(Fe,Mn)_2SiO_4$ could hinder the reduction process much more [19]. It is noted that the effect of the gangue species on the reduction kinetics can depend on the atmosphere. In nitrogen gas, Basumallick [62] observed that minor addition of CaO (0.6–1.2 mass%) has no influence on the reaction degree of haematite-lignite mixed pellets at 1173–1273 K. In the reduction experiments at low temperatures (1173–1473 K), Prasannan et al. [63] developed a mathematical modelling to investigate the effect of addition to the reduction. They suggested that optimal inert addition content can improve the solid reactivity.

Although different conclusions were made in the previous works, based on them, it could be summarized that the reduction rate acceleration of doped iron oxide is due to:

(1) Basicity of gangue and solubility of them in slag;
(2) Formation of intermediate oxides which can be easily reduced compared to iron oxide;
(3) Higher porosity of the raw materials;
(4) Disorder of oxide lattice;
(5) The reduction of raw materials to alloy rather than pure iron, which reduces the reaction energy barrier.

Conclusions

High-temperature reduction of iron oxide particles in suspension is used in alternative ironmaking processes. The phase transformation and kinetics study of the haematite and magnetite suspension reduction above 1473 K are reviewed in this work. Three characteristics were summarized as follows:

(1) Thermal decomposition of haematite is the principal reaction in the high-temperature reduction of suspension;
(2) The reduction rate constant of iron oxides suspension is from 10^{-2} to 10^0 s^{-1}, so that the reaction reaches the end point within seconds in the reactor;
(3) melting of particles is accompanied with retardation of the suspension reduction process.

Topochemical reaction of the particles has been observed in previous studies. These studies indicated that the proper kinetic model to describe the reduction of iron oxides suspension could be the un-reacted core shrinking model with chemical reaction rate determining step or the kinetic form of $[-\ln(1-x)]^{1/n}$ with varying values of n. The activation energy of haematite and magnetite reduction was reported to be from 45 to 594 kJ mol^{-1}.

Iron ore particles can contain gangue minerals in the grain, which could affect the phase transformation and kinetics in the reduction. Although some rough projections and estimates could be extracted from the current studies, more investigations are required in the near future.

ORCID

Zhiyuan Chen 🔟 http://orcid.org/0000-0002-7993-7386
Yongxiang Yang 🔟 http://orcid.org/0000-0003-4584-6918

References

[1] Meijer K, Denys M, Lasar J, et al. ULCOS: ultra-low CO_2 steelmaking. Ironmak Steelmak. 2009;36(4):249–251.
[2] Sohn H, Moo EC, Zhang Y, et al.2009). Suspension reduction technology for ironmaking with low CO2 emission and energy requirement. Iron and Steel Technology Conference, AISTech 2009.
[3] Choi M, Sohn H. Development of green suspension ironmaking technology based on hydrogen reduction of iron oxide concentrate: rate measurements. Ironmak Steelmak. 2013;37(2):81–88.
[4] Sohn HY, Mohassab Y. Development of a novel flash ironmaking technology with greatly reduced energy consumption and CO_2 emissions. J Sustain Metal. 2016;2(3):216–227. doi:10.1007/s40831-016-0054-8.
[5] Park W-I, Jung S-M. Effective use of CH_4 gas as a reducing agent in suspension reduction process. ISIJ Int. 2015;55(1):166–174. doi:10.2355/isijinternational.55.166.
[6] Xu J, Wang N, Chen M, et al. Reduction behavior of blast furnace dust particles during in-flight processes. Ind Eng Chem Res. 2018;57(1):111–121. doi:10.1021/acs.iecr.7b03849.
[7] Xu J, Xin J, Wang N, et al. editors. Kinetic analysis of blast furnace dust recycling with flash reduction process at high temperature. Cham: Springer International; 2018 (9th International Symposium on high-temperature metallurgical processing).
[8] Sundman B. An assessment of the Fe-O system. J Phase Equilib. 1991;12(2):127–140.
[9] Fabrichnaya O, Sundman B. The assessment of thermodynamic parameters in the Fe-O and Fe-Si-O systems. Geochim Cosmochim Acta. 1997;61(21):4539–4555.
[10] Qu Y, Yang Y, Zou Z, et al. Melting and reduction behaviour of individual fine hematite ore particles. ISIJ Int. 2015;55(1):149–157. doi:10.2355/isijinternational.55.149.
[11] Qu Y, Yang Y, Zou Z, et al. Thermal decomposition behaviour of fine iron ore particles. ISIJ Int. 2014;54(10):2196–2205.
[12] Qu Y, Yang Y, Zou Z, et al. Reduction kinetics of fine hematite Ore particles with a high temperature drop tube furnace. ISIJ Int. 2015;55(5):952–960. doi:10.2355/isijinternational.55.952.
[13] Hayes P, Grieveson P. Microstructural changes on the reduction of hematite to maanetite. Metall Trans B. 1981;12(3):579–587.
[14] Swann P, Tighe N. High voltage microscopy of the reduction of hematite to magnetite. Metall Trans B. 1977;8(2):479–487.

[15] Kashiwaya Y, Yamaguchi Y, Kinoshita H, et al. In situ observation of reduction behavior of hematite with solid carbon and crystallographic orientation between hematite and magnetite. ISIJ Int. 2007;47(2):226–233.

[16] Gudenau HW, Senk D, Wang S, et al. Research in the reduction of iron ore agglomerates including coal and C-containing dust. ISIJ Int. 2005;45(4):603–608. doi:10.2355/isijinternational.45.603.

[17] Baguley P, John DHS, Hayes P. The conditions for the formation of lath and porous magnetite on reduction of hematite in H_2/H_2O gas mixtures. Metall Mater Trans B. 1983;14(3):513–514.

[18] Komatina M, Gudenau HW. The sticking problem during direct reduction of fine iron ore in the fluidized bed. Metalurgija. 2004;10(4):309–328.

[19] El-Geassy AA, Nasr MI, Mousa EA. Influence of manganese oxide and silica on the morphological structure of hematite compacts. Steel Res Int. 2010;81(3):178–185. doi:10.1002/srin.200900121.

[20] Wong P, Kim M, Kim H, et al. Sticking behaviour in direct reduction of iron ore. Ironmak Steelmak. 2013;26(1):53–57.

[21] Seaton CE, Foster JS, Velasco J. Structural changes occurring during reduction of hematite and magnetite pellets containing coal char. Trans Iron Steel Inst Japan. 1983;23(6):497–503. doi:10.2355/isijinternational1966.23.497.

[22] Muan A. Phase equilibria at high temperatures in oxide systems involving changes in oxidation states. Am J Sci. 1958;256(3):171–207.

[23] Sohn HY, Chaubal PC. The ignition and combustion of chalcopyrite concentrate particles under suspension-smelting conditions. Metall Trans B. 1993;24(6):975–985. doi:10.1007/BF02660989.

[24] Nakamoto M, Ono-Nakazato H, Kawabata H, et al. Reduction behavior of wustite compact with pore blockade by liquid slag. Tetsu-to-Hagane. 2004;90(1):1–8.

[25] Maeda T, Ono Y. Reduction equilibria of ternary calcium ferrite with $CO-CO_2$ gas mixture. Tetsu-to-Hagane. 1994;80(6):451–456.

[26] Ono Y, Murayama T, Maeda T. Reduction equilibria of multi-component calcium ferrite with CO-CO2 gas mixture. Trans Iron Steel Soci AIME. 1991;12:115–123.

[27] Bradshaw AV, Matyas AG. Structural changes and kinetics in the gaseous reduction of hematite. Metall Trans B. 1976;7(1):81–87. doi:10.1007/BF02652822.

[28] Valipour M. Mathematical modeling of a non-catalytic gas-solid reaction: hematite pellet reduction with syngas. Scientia Iranica. 2009;16:108–124.

[29] Wen C. Noncatalytic heterogeneous solid-fluid reaction models. Ind Eng Chem. 1968;60(9):34–54.

[30] Turkdogan E, Vinters J. Gaseous reduction of iron oxides: part I. Reduction of hematite in hydrogen. Metall Mater Trans B. 1971;2(11):3175–3188.

[31] Tsukihashi F, Kato K, Otsuka K-I, et al. Reduction of molten iron oxide in CO gas conveyed system. Tetsu-to-Hagane. 1982;68(7):750–758.

[32] Tsukihashi F, Kato K, Otsuka K-I, et al. Reduction of molten iron oxide in CO gas conveyed system. Trans Iron Steel Inst Japan. 1982;22(9):688–695. doi:10.2355/isijinternational1966.22.688.

[33] Hayashi S, Iguchi Y. Influence of gangue species on hydrogen reduction rate of liquid wustite in gas-conveyed systems. ISIJ Int. 1995;35(3):242–249.

[34] Takeuchi N, Nomura Y, Ohno K-I, et al. Kinetic analysis of spherical wustite reduction transported with CH_4 gas. Tetsu-to-Hagane. 2009;94(4):115–120.

[35] Warner NA. Towards zero CO2 continuous steelmaking directly from ore. Metall Mater Trans B. 2014 2014;45(6):2080–2096. doi:10.1007/s11663-014-0136-6.

[36] Takeuchi N, Nomura Y, Ohno K-I, et al. Kinetic analysis of spherical wuestite reduction transported with CH4 gas. ISIJ Int. 2007;47(3):386–391.

[37] Nomura Y, Nakagawa H, Maeda T, et al. Rapid reduction of fine iron ore transported with CH_4 gas. Tetsu-to-Hagane. 2005;91(6):521–527.

[38] Hayashi S, Iguchi Y. Hydrogen reduction of liquid iron oxide fines in gas-conveyed systems. ISIJ Int. 1994;34(7):555–561. doi:10.2355/isijinternational.34.555.

[39] Fan D, Mohassab Y, Elzohiery M, et al. Analysis of the hydrogen reduction rate of magnetite concentrate particles in a drop tube reactor through CFD modeling. Metall Mater Trans B. 2016;47(3):1669–1680. doi:10.1007/s11663-016-0603-3.

[40] Fan D-Q, Sohn HY, Elzohiery M. Analysis of the reduction rate of hematite concentrate particles in the solid state by H2 or CO in a drop-tube reactor through CFD modeling. Metall Mater Trans B. 2017;48(5):2677–2684. doi:10.1007/s11663-017-1053-2.

[41] Abolpour B, Afsahi MM, Soltani Goharrizi A, et al. Simulating reduction of in-flight particles of magnetite concentrate by carbon monoxide. Ironmak Steelmak. 2017;44(10):750–761. doi:10.1080/03019233.2016.1232879.

[42] Abolpour B, Afsahi MM, Soltani Goharrizi A, et al. Investigation of in-flight reduction of magnetite concentrate by hydrogen. Ironmak Steelmak. 2017;44:1–11.

[43] Guo L, Gao J, Zhong Y, et al. Flash suspension reduction of ultra-fine Fe_2O_3 powders and the kinetic analyzing. ISIJ Int. 2015;55(9):1797–1805.

[44] Salmani M, Alamdari EK, Firoozi S. Isoconversional analysis of thermal dissociation kinetics of hematite in air and inert atmospheres. J Therm Anal Calorim. 2017;128(3):1385–1390.

[45] Qu Y. (2013). Experimental study of the melting and reduction behaviour of ore used in the HIsarna process (PhD thesis). Delft University of Technology.

[46] Choi ME. Suspension hydrogen reduction of iron ore concentrate. Salt Lake City: The University of Utah; 2010.

[47] Ramachandran P, Doraiswamy L. Modeling of noncatalytic gas-solid reactions. AIChE J. 1982;28(6):881–900.

[48] Wang H. Reduction kinetics of iron ore concentrate particles relevant to a novel green ironmaking process. Salt Lake City: The University of Utah; 2011.

[49] Wang H, Sohn H. Hydrogen reduction kinetics of magnetite concentrate particles relevant to a novel flash ironmaking process. Metall Mater Trans B. 2013;44(1):133–145.

[50] Elzohiery M, Sohn HY, Mohassab Y. Kinetics of hydrogen reduction of magnetite concentrate particles in solid state relevant to flash ironmaking. Steel Res Int. 2017;88(2):1600133–n/a. doi:10.1002/srin.201600133.

[51] Chen F, Mohassab Y, Zhang S, et al. Kinetics of the reduction of hematite concentrate particles by carbon monoxide relevant to a novel flash ironmaking process. Metall Mater Trans B. 2015;46(4):1716–1728. doi:10.1007/s11663-015-0345-7.

[52] Chen F, Mohassab Y, Jiang T, et al. Hydrogen reduction kinetics of hematite concentrate particles relevant to a novel flash ironmaking process. Metall Mater Trans B. 2015;46(3):1133–1145. doi:10.1007/s11663-015-0332-z.

[53] Mohassab Y, Chen F, Elzohiery M, et al. Reduction kinetics of hematite concentrate particles by CO + H2 mixture relevant to a novel flash ironmaking process. In: Hwang J-Y, Jiang T, Pistorius PC, et al. editor. 7th International Symposium on high-temperature metallurgical processing. Cham: Springer International; 2016. p. 221–228.

[54] Abolpour B, Afsahi MM, Azizkarimi M. Reduction kinetics of magnetite concentrate particles by carbon monoxide. Min Proc Extractive Metall. 2018;127(1):29–39.

[55] Wang H, Sohn HY. Reduction of magnetite concentrate particles by H_2+CO at 1673K. ISIJ Int. 2015;55(3):706–708.

[56] Nagasaka T, Hino M, Ban-Ya S. Interfacial kinetics of hydrogen with liquid slag containing iron oxide. Metall Mater Trans B. 2000;31(5):945–955.

[57] Nasr MI, Omar AA, Khedr MH, et al. Effect of nickel oxide doping on the kinetics and mechanism of iron oxide reduction. ISIJ Int. 1995;35(9):1043–1049. doi:10.2355/isijinternational.35.1043.

[58] El-Geassy AA. Gaseous reduction of MgO-doped Fe_2O_3 compacts with carbonmonoxide at 1173-1473K. ISIJ Int. 1996;36(11):1328–1337. doi:10.2355/isijinternational.36.1328.

[59] El-Geassy A. Influence of doping with CaO and/or MgO on stepwise reduction of pure hematite compacts. Ironmak Steelmak. 1999;26(1):41–52.

[60] El-Geassy A-HA, Nasr MI, Omar AA, et al. Reduction kinetics and catastrophic swelling of MnO_2-doped Fe_2O_3 compacts with CO at 1073-1373K. ISIJ Int. 2007;47(3):377–385. doi:10.2355/isijinternational.47.377.

[61] El-Geassy A-HA, Nasr MI, Omar AA, et al. Influence of SiO_2 and/or MnO_2 on the reduction behaviour and structure changes of Fe_2O_3 compacts with CO gas. ISIJ Int. 2008;48(10):1359–1367. doi:10.2355/isijinternational.48.1359.

[62] Basumallick A. Influence of CaO and Na_2CO_3 as additive on the reduction of hematite-lignite mixed pellets. ISIJ Int. 1995;35(9):1050–1053. doi:10.2355/isijinternational.35.1050.

[63] Prasannan PC, Ramachandran PA, Doraiswamy LK. A model for gas-solid reactions with structural changes in the presence of inert solids. Chem Eng Sci. 1985;40(7):1251–1261. doi:10.1016/0009-2509(85)85084-3.